Journal of Mines, Metals and Fuels, *71(12A): 27-37; 2023. DOI: 10.18311/jmmf/2023/45494*

Print ISSN : 0022-2755

Journal of Mines, Metals and Fuels

Contents available at: *www.informaticsjournals.com/index.php/jmmf*

CFD Approach to Evaluate Pin-Fin Performance for Forced Convection Heat Transfer

Ayush Naman, Ayush Kamle, Kanishk Sahu and K. G. Nithesh*

Mechanical Engineering Department, Siddaganga Institute of Technology, Tumkur - 572103, Karnataka, India; nitheshkg@sit.ac.in

Abstract

In the digital age, fins are often used as effective elements for heat transfer enhancement, extending the life and efficiency of devices while achieving superior thermal management and high performance. Understanding forced convection through fins provides valuable insights for optimizing heat management in many industries such as aviation, heat exchangers, electronic equipment, IC engines, and underground mine ventilation system applications. The current research focuses on the flow and heat transfer characteristics of Pin-Fin using CFD and theoretical approach. A pin fin model for forced convection has been designed and held horizontally inside the rectangular duct in this investigation. The pin fin is made of Brass and measures 1.2 cm in diameter and 12 cm in length. The Fin is enclosed by a 15cm x 10cm x 100cm rectangular duct. The objective of this research work is to make a comparison of the heat transfer coefficient, fin efficiency, and efficacy at various Reynolds numbers to analytical values. ANSYS Geometry is used to create the three-dimensional model, which is then meshed by ANSYS Mesh. The CFX solver is used to obtain CFD results. The outcome of the CFD simulation is in good agreement with analytical approach.

Keywords: *CFD, Duct, Forced Convection, Pin-Fin*

1.0 Introduction

Thermal management is becoming an increasingly significant feature of electronic product design as heat dissipation from microelectronics devices increase[1]. Excess heat from the device must be transmitted to the environment in order to attain the desired component temperature[2]. Heat transfer can be improved in a variety of different ways, including through the use of active, passive, and compound augmentation approaches. For active methods, some kind of power from outside the system is needed, usually from the fluid moving through the heat exchanger to the wall. If the power comes from the flow of the fluid itself, it is possible to use the instability of the flow to make the heat transfer coefficient higher. Passive enhancements do not need any external power to function. Passive enhancing methods include treated, rough, extended, displaced, swirl flow, coiled tubes, surface tension, and fluid additives. Compound enhancement is when two or more of these approaches are used together to improve heat transfer more than when used individually[3]. Numerous studies have already established that fins are a thermal management method that increases the available surface area and hence the total heat dissipation[4].

Pin-fins fitted on a heat exchanger surface can increase the heat transfer surface area and induce turbulent flow mixing, enhancing heat transfer performance and prolonging the life of the device[5,6]. Finned surfaces are used to cool electronic components, thermal power plant components, cooling towers, IC engines, and R&AC evaporators and condensers[7]. Finned pins improve heat transfer by 85% and effectiveness by 61%[8]. Steady-state heat transfer from pin-fin arrays has been

*Author for correspondence

experimentally studied for staggered and in-line layouts. The Nusselt number's (in both directions) dependences on the Reynolds number and pin-fin pitch have been computed[5]. A finned surface is fitted to a rectangular duct that uses air as the working fluid at 45 °C. Depending on the hydraulic diameter, the Reynolds number (3700 to 30000) was chosen as the variables. With the staggered array, a 33 percent increase in heat transfer at constant pumping power was accomplished[9]. A transitional airflow in a rectangular channel with staggered arrays of short pin fins was investigated experimentally. Researchers calculate transitional flow friction factors, average Nusselt numbers, and thermal performance. Pin fins enhance heat transfer[10]. The researcher found an experimental model for forced convection pin fin heat sinks. CFD simulations validated empirical data and correlations for thermal resistance and heat transfer in circular pin fin arrays. CFD analyses design parameters including height diameter and pin-fin spacing[11]. The Pin fins, according to the author, are useful for enhancing heat transmission while retaining a reasonable level of performance[7].

One-dimensional heat transfer problems that can be approached using several techniques were discussed. The approximate solution was verified using an analytical approach based on direct solutions of differential equations. The insulated fin tip was used in this investigation[12]. Computerized numerical analysis of air flow and heat transfer in a lightweight vehicle engine with three pin fin morphologies is presented[13]. Shape, spacing, height, base thickness, material type, and surface fins affect fin selection. Heat transfer and pressure drop channels with circular extended surface have been studied extensively. Heat transfer rises with airflow. The heat transfer coefficient increases as the velocity of air increases because the fin spends less time in contact with the air, resulting in reduced real heat transfer and fin efficiency in forced convection[14]. The study examines the heat transfer performance of a heat sink at 308K, 323K, 338K, 353K, and 368K. Thermal resistance was affected by porosity between 0.524 and 0.960. The heat transfer coefficient rises when the heat sink and ambient temperatures differ[15]. Chamoli S. *et al*. used Computational Fluid Dynamics to study heat transfer and friction loss in a horizontal rectangular channel with circular profile fins 5cm height and 2cm diameter attached to one heated surface. The Reynolds number ranged from 5000 to 30,000 based on the flow averaged inlet velocity and hydraulic diameter are considered. The Reynolds number, fin arrangement, and fin pitch are numerical parameters for the analysis[16].

Experiments were conducted to verify the fluid flow and heat transfer properties of a fin array with lateral circular holes and its outside dimensionally equivalent solid fin arrays. The purpose of these experiments was to find a solution to a problem involving natural convection. ANSYS 12.0 fluid flow (CFX) has been used[17]. This research investigates pin fin convective heat transfer in natural and forced modes. The cylindrical pin fin was used in the pin fin apparatus experiment. During both forms of convective heat transfer, the fluctuations in several parameters were observed. This research aided in the comparison of natural and forced convective heat transfer through pin fins[18]. PhD Thesis of Andrew Gordon Watson has demonstrated the nature and magnitude of the contribution of conveyed coal to the total underground heat load. Heat transfer through broken coal is examined and this article describes a duct-based conveyor model for the underground mines[19]. Computational fluid dynamics is one of the major tools used to study the air-flow distribution required for adequate ventilation of underground mining[20,21]. The convective heat transfer coefficient of ventilation air in a potash mine is evaluated in the article by de Felipe[22]. Sources of heat linked to mining operations are discussed by Wagner[23]. Underground mines often have ventilation systems to provide fresh air and remove pollutants. This existing airflow can be leveraged for forced convection cooling. Understanding forced convection through fins provides valuable insights for optimizing heat management in underground mining applications. We observed that heat dissipation and thermal management approaches are continually in demand in industries such as aviation, heat exchangers, electronic equipment, IC engines, underground mining and so on, after completing a thorough literature review. Numerous research has shown that extended surfaces or fins can be used effectively and widely in a variety of scenarios. The coefficients of convective heat transfer, the temperature of the system and the working fluid, wetted surface area of the extended surfaces are factors that have an impact on the rate of heat transfer.

This study investigates flowing fluid convective heat transfer coefficients using 3D steady RANS CFD simulations of forced convective heat transfer for a 1.2 cm-diameter, 12-cm-long brass fin held horizontally inside a 15cmX10cmX100cm rectangular duct.

2.0 Methodology

In this research work we have carried out both analytical and CFD approach to analyse the Pin Fin heat transfer performance under forced convection heat transfer.

2.1 Analytical Approach

A straight circular fin protrudes from a wall surface shown in Figure 1. Let the wall surface be at temperature T_s which is higher than the surrounding air temperatureT_∞. The fin is cooled along its surface by the ambient air at a temperatureT_∞. The fin has a uniform cross-sectional area A_c, perimeter P, length L and thickness 2_δ. Spin with circular profile has diameter d. The heat transfer coefficient between the surface of the fin and the fluid is h.

For the analysis of heat flow through the fin the following assumptions are made:

(a) The fin material is homogeneous and isotropic; hence the thermal conductivity of the fin material is uniform.

(b) The temperature at any cross-section of the fin is uniform i.e. T= T (x) only. In other words, the heat conduction is one- dimensional.

(c) The heat transfer coefficient **h** is uniform over the entire surface.

(d) There is no heat generation.

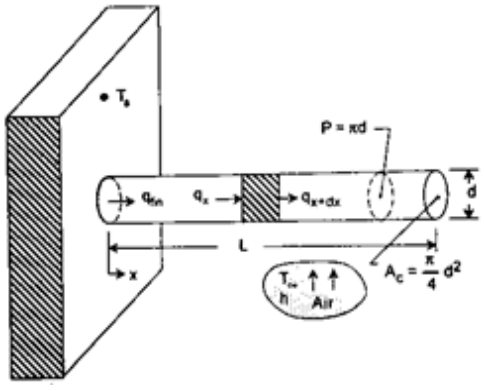

Figure 1. Pin Fin Profile[24].

(e) Contact thermal resistance is negligible.

(f) Radiation is negligible.

(g) The heat conduction is steady state.

An infinitesimal fin or spine element of length *dx* at *x* from the wall base. Under steady state conditions, heat flow into and out of the element is equal. In other words,

Heat conducted at *x* = Heat conducted at *(x + dx)* +Heat convected between *x* and *(x + dx)*

Or $q_x = q_{x+dx} + q_{conv}$ (1)

Heat conducted at $x = q_x = -kA_c\frac{dT}{dx}$

Heat conducted at

$$x + dx \; -kA_c\frac{dT}{dx} + \frac{d}{dx}(-kA_c\frac{dT}{dx})dx$$

Heat convected from length

$$\mathrm{dx} = \mathrm{q_{conv}} = h.A_s(T-T_\infty). = h.Pdx(T-T_\infty)$$

where *P* perimeter of the element,

A_s Surface area $= P.\,dx$

Putting the value of q_x, q_{x+dx} and q_c into the equation (1), we get

$$-kA_c\frac{dT}{dx} = -kA_c\frac{dT}{dx} + \frac{d}{dx}\left(-kA_c\frac{dT}{dx}\right)dx$$
$$+h.Pdx(T-T_\infty)$$
$$\text{Or } \frac{d}{dx}\left(-kA_c\frac{dT}{dx}\right)dx + hP\,dx(T-T_\infty) = 0$$
$$\text{Or } \frac{d}{dx}\left(-kA_c\frac{dT}{dx}\right) + hP(T-T_\infty) = 0$$
$$\text{Or } \frac{d^2T}{dx^2} = \frac{\mathrm{hP}}{kA_c}(\mathrm{T}-T_\infty)$$
$$\text{Or } \frac{d^2T}{dx^2} = \mathrm{m}^2(\mathrm{T}-T_\infty) \quad (2)$$

Where $\mathrm{m} = \sqrt{\frac{h.P}{kA_c}} = \text{constant}$

The constant "m" has the physical significance

That $\mathrm{mL} = \sqrt{\frac{h.P}{kA_{c/L}}} = \left[\frac{\text{Surface conductance}}{\text{Internal conductance}}\right]^{\frac{1}{2}}$

The equation (2) is the *second order linear differential equation*. Its solution may he found by assuming temperature excess as $\theta = (T-T_\infty)$

Hence, the equation (2) becomes $\frac{d^2\theta}{dx^2} = \mathrm{m}^2\theta$

The general solution is

$$\theta = (\mathrm{T} - T_\infty) = C_1 e^{mx} + C_2 e^{-mx} \quad (3)$$

The constants C_1 and C_2 may be obtained by using the suitable boundary conditions. Several boundary conditions are considered here as follows that will depend upon the nature of the problems.

Insulated End: The temperature gradient is zero at the end of a finite-length fin with insulation. Hence, the boundaries for this situation are

(i) $x = 0,\ T = T_s$ *, i.e.,* $\theta = \theta_s$*, and (ii) At* $x = L, \frac{d\theta}{dx} = 0$

Using these two boundary conditions to equation (3), we get

$$\theta_s = T_s - T_\infty = C_1 + C_2$$

And $C_1 e^{mL} - C_2 e^{-mL} = 0$

Solving the above two equations, we get

$C_1 = \frac{\theta_s}{1+e^{2mL}}$ and $C_2 = \frac{\theta_s}{1+e^{-2mL}}$

Substituting the constants C_1 and C_2 into equation (3), we get

$$\frac{\theta}{\theta_s} = \frac{T - T_\infty}{T_s - T_\infty} = \frac{e^{mx}}{1 + e^{2mL}} + \frac{e^{-mx}}{1 + e^{-2mL}}$$

Or $\frac{\theta}{\theta_s} = \frac{\cosh m(L-x)}{\cosh mL}$

The rate heat flow from the fin is obtained as

$$q_{fin} = -kA_c\left(\frac{d\theta}{dx}\right)_{x=0} = kA_c m\theta_s \tanh mL$$

$$q_{fin} = \sqrt{(hPkA_c)}\theta_s \tanh mL$$

2.2 CFD Approach

The ANSYS CFX tool was used to improve forced convection heat transfer and reduce friction factor. It uses the SST model to solve the three-dimensional Navier-Stokes equations for steady-state turbulent flow and to improve wall treatment. At fully developed velocity and temperature, the numerical analysis was provided. Continuity, Navier–Stokes, and thermal energy are the governing equations for flow and heat transfer, as written below[25].

Continuity equation:

$$\frac{\partial}{\partial x}(\rho V_x) + \frac{\partial}{\partial y}(\rho V_y) + \frac{\partial}{\partial z}(\rho V_z) = 0$$

Momentum equation:

$$\frac{\partial}{\partial x}(\rho V_x V_x) + \frac{\partial}{\partial y}(\rho V_y V_x) + \frac{\partial}{\partial z}(\rho V_z V_x) = \rho g_x - \frac{\partial P}{\partial x} + \frac{\partial}{\partial x}\left(\mu_e \frac{\partial V_x}{\partial x}\right) + \frac{\partial}{\partial y}\left(\mu_e \frac{\partial V_x}{\partial y}\right) + \frac{\partial}{\partial z}\left(\mu_e \frac{\partial V_x}{\partial z}\right) + T_x$$

$$\frac{\partial}{\partial x}(\rho V_x V_y) + \frac{\partial}{\partial y}(\rho V_y V_y) + \frac{\partial}{\partial z}(\rho V_z V_y) = \rho g_y - \frac{\partial P}{\partial y} + \frac{\partial}{\partial x}\left(\mu_e \frac{\partial V_y}{\partial x}\right) + \frac{\partial}{\partial y}\left(\mu_e \frac{\partial V_y}{\partial y}\right) + \frac{\partial}{\partial z}\left(\mu_e \frac{\partial V_y}{\partial z}\right) + T_y$$

$$\frac{\partial}{\partial x}(\rho V_x V_z) + \frac{\partial}{\partial y}(\rho V_y V_z) + \frac{\partial}{\partial z}(\rho V_z V_z) = \rho g_z - \frac{\partial P}{\partial z} + \frac{\partial}{\partial x}\left(\mu_e \frac{\partial V_z}{\partial x}\right) + \frac{\partial}{\partial y}\left(\mu_e \frac{\partial V_z}{\partial y}\right) + \frac{\partial}{\partial z}\left(\mu_e \frac{\partial V_z}{\partial z}\right) + T_z$$

Energy equation:

$$\frac{\partial}{\partial x}(\rho V_x C_p T) + \frac{\partial}{\partial y}(\rho V_y C_p T) + \frac{\partial}{\partial z}(\rho V_z C_p T) = \frac{\partial}{\partial x}\left(K \frac{\partial T}{\partial x}\right) + \frac{\partial}{\partial y}\left(K \frac{\partial T}{\partial y}\right) + \frac{\partial}{\partial z}\left(K \frac{\partial T}{\partial z}\right)$$

This study uses SST turbulence model. SST turbulence model combines k-ε and k- ω characteristics.

2.3 Computational Domain with Boundary Conditions

A pin fin model for forced convection has been designed and held horizontally inside the rectangular duct in this investigation. The pin fin is made of Brass and measures 1.2 cm in diameter and 12 cm in length. The Fin is enclosed by a rectangular duct measuring 15 cm X 10 cm X 100 cm. The Figures 2-5 shows the computational domain employed for modelling of duct and fin surface in

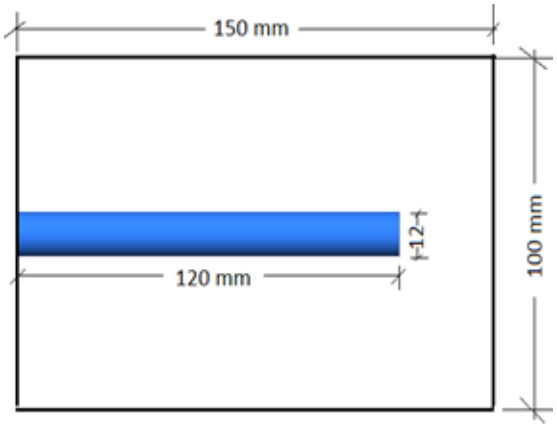

Figure 2. Schematic display of duct-fin assembly.

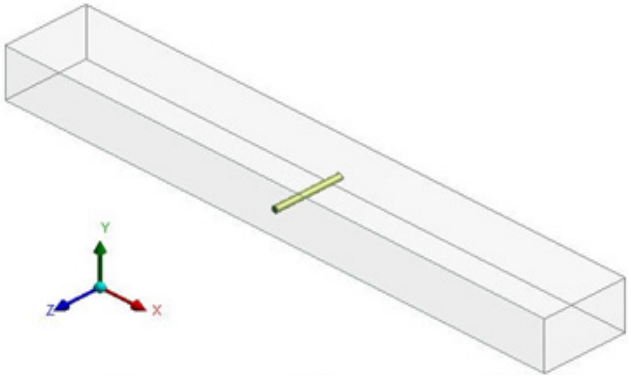

Figure 3. 3D model of duct-fin assembly.

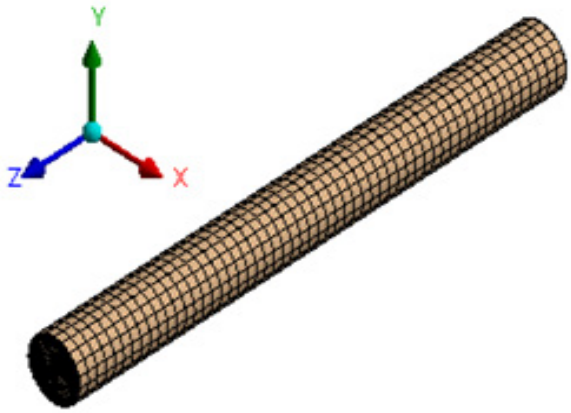

Figure 4. Meshing of fin.

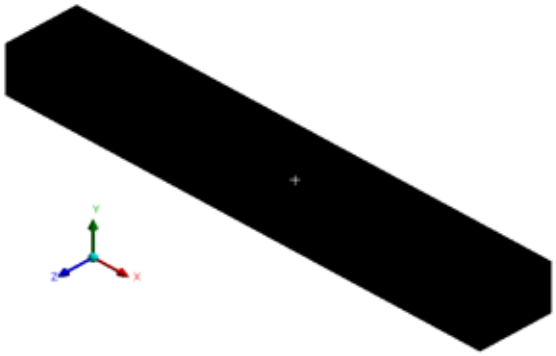

Figure 5. Meshing of duct.

Table 1. CFD setup and boundary conditions

Analysis type	**Steady state**	
Domains	**Duct and fin**	
Duct	Inlet	Outlet
	Velocity is 0.2m/s Temperature is 39˚C	Mass flow rate is 0.003393 kg/s
Fin	Base temperature is 105˚C Tip is insulated	

steady flow condition. ANSYS Geometry is used to create the three-dimensional model, which is then meshed by ANSYS Mesh.

The CFD setup and boundary condition is given as shown in the Table 1. An air is chosen as a working fluid flowing through the duct. The pin fin is made of Brass having thermal conductivity of 110.48 W/mK is selected for the simulation. Heat source with base temperature of 105˚C is given at the bottom of the fin. The CFX solver is used to obtain CFD results.

3.0 Results and Discussion

The current investigation includes both analytical and CFD approach to evaluate the performance of Pin Fin held horizontally inside the duct for a forced convection heat transfer. The analytical results have been evaluated, and the work has been simulated using CFD.

3.1 CFD Simulation Results

We have carried out the CFD simulation for various cases by varying the velocity of working fluid.

This Figure 6 shows temperature variation in Pin Fin as fin base has higher temperature of 378 Kelvin. Figure 6 illustrates the decrease in temperature from the base to the tip of the fin. The air temperature passing over the fin at a velocity of 0.1 m/s is 312 Kelvin. Convection causes the temperature of the fin to decrease as the rate of heat transfer increases when air passes over its surface.

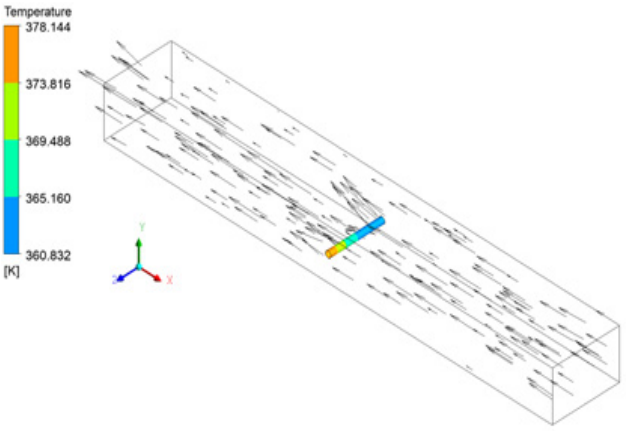

Figure 6. Pin fin temperature distribution with 0.1m/s air velocity (Case-1).

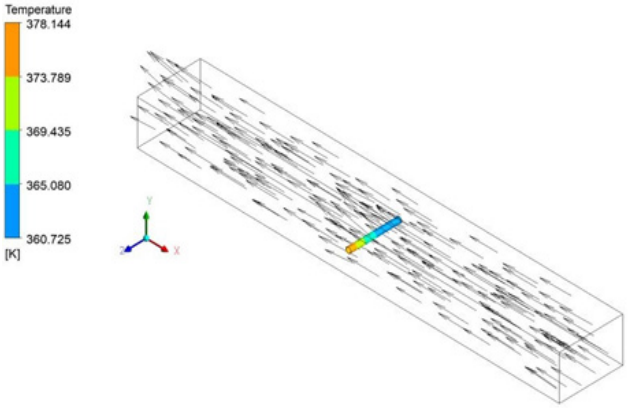

Figure 7. Pin fin temperature profile at 0.2m/s air velocity (Case-2).

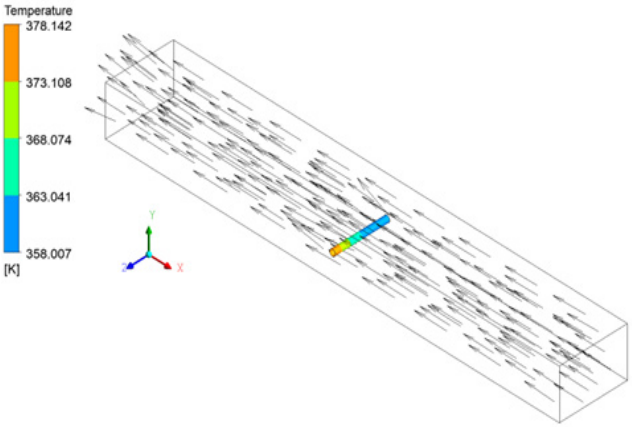

Figure 8. Temperature profile of pin fin at 0.3m/s air velocity (Case-3).

The temperature distribution in the Pin Fin is illustrated in Figure 7, where the fin base has a higher temperature of 378 Kelvin. Figure 7 illustrates the decrease in temperature from the base to the tip of the fin. The air velocity passing over the fin is 0.2 m/s, and the corresponding air temperature is 312 Kelvin. Convection enhances heat transfer rate and reduces the fin temperature when air passes across its surface.

The Figure 8 plot illustrates the temperature distribution of Pin Fin, where the fin base exhibits a

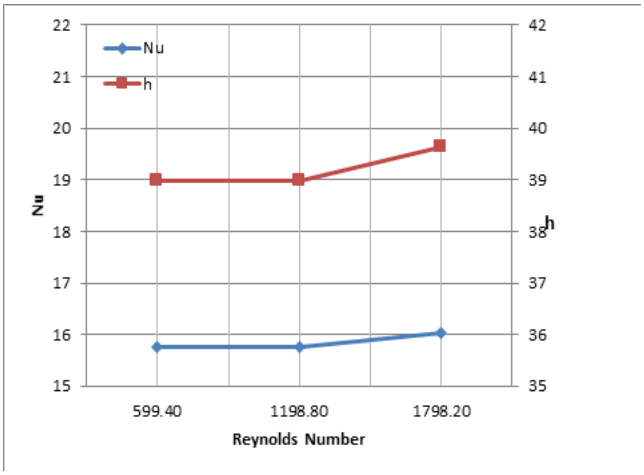

Figure 9. Nusselt number and convection heat transfer coefficient vs Reynolds number.

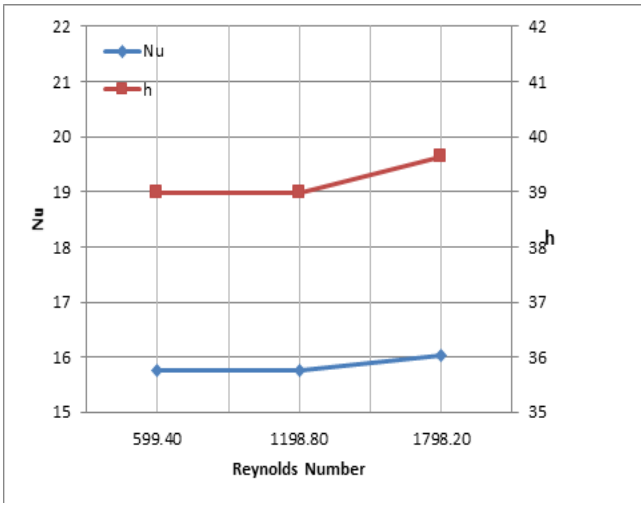

Figure 10. Fin efficiency and effectiveness vs Reynolds number.

higher temperature of 378 Kelvin. Figure 8 illustrates the decrease in temperature from the base to the tip of the fin. The air velocity travelling over the fin is 0.3 m/s, and the corresponding air temperature is 312 Kelvin. Convection enhances heat transfer and causes the temperature of the fin to decrease as air passes over its surface.

The temperature distribution across the fin for three different cases shows that with increase in flowing fluid (air) velocity (0.1 m/s, 0.2 m/s, 0.3m/s) the temperature in three cases at various equivalent locations in the fin decreases.

The Reynolds numbers for Case 1, Case 2, and Case 3, as determined by CFD simulation, are 599.4, 1198.8, and 1798.20, respectively. Figure 9 illustrates the relationship between the Nusselt number, which represents the convective heat transfer, and the Reynolds number in the Pin Fin. The Figure illustrates that the Nusselt number rises in correlation with the Reynolds number, indicating an enhanced heat transmission capability in the pin fin. This enhancement is further amplified by an increase in the convection coefficient (h).

The thermal performance of the fin diminishes as the Reynolds number (Figure 10) increases. As the fluid velocity increases, the duration of contact between the fin and the air reduces, leading to a decrease in the overall thermal efficiency of the fin in forced convection.

3.2 Analytical Results

We conducted theoretical calculations for different scenarios by altering the velocity of the working fluid. The Reynolds numbers for Case 1, Case 2, and Case 3, as determined by an analytical approach, are 632.58, 1265.16, and 1897.73, respectively.

The Nusselt number and convection heat transfer coefficient in the Pin Fin have been plotted as functions of the Reynolds number in Figure 11. The Nusselt number increases with the Reynolds number, and the heat transmission capability in the pin fin increases as

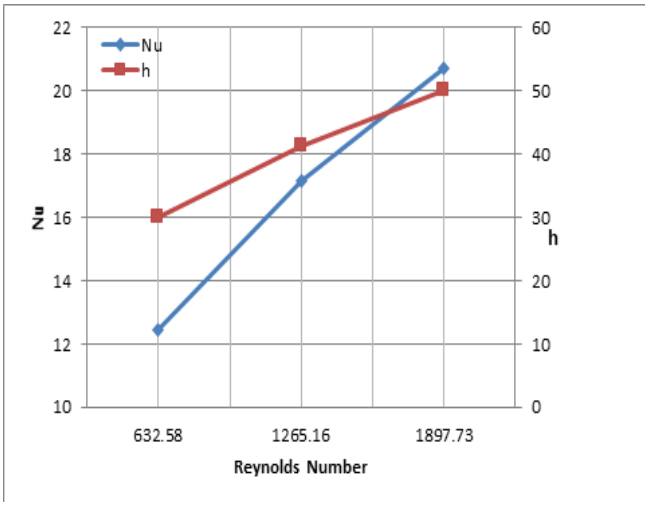

Figure 11. Nusselt number and convection heat transfer coefficient vs Reynolds number.

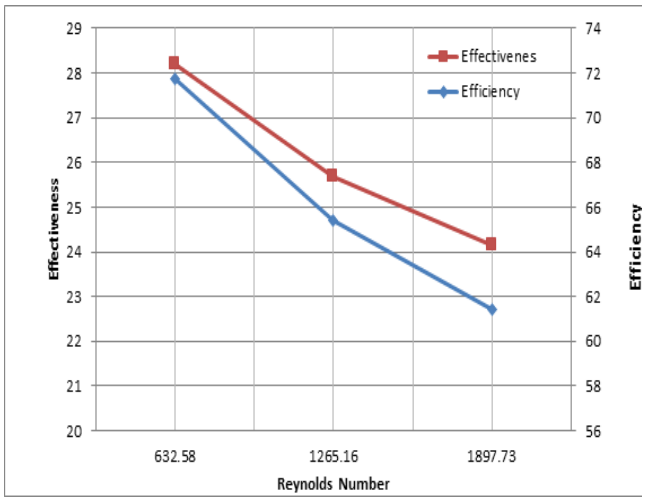

Figure 12. Fin Efficiency and Effectiveness Vs Reynolds Number

the convection coefficient (h) increases, as depicted in Figure 11.

The duration of contact between the fin and the air decreases as the velocity of the flowing fluid increases, leading to a decline in the overall thermal efficiency of the fin in forced convection, as depicted in Figure 12.

3.3 Comparison and Validation of CFD Results with Analytical Results

We have taken base temperature from CFD to calculate the temperature distribution at different locations of the fin for Theoretical analysis. Tables 2-4 shows the comparison of temperature distribution at 0.1 m/s (Case 1), 0.2 m/s (Case 2) and 0.3m/s (Case 3), respectively.

Table 2 shows that at 0.1 m/s velocity, the error values of T2, T3, T4, and T5 for theoretical and CFD findings are 8.5 per cent, 8.5 per cent, 13.5 per cent, and 19.1 per cent, respectively.

Table 3 shows that at 0.2 m/s velocity, the error values of T2, T3, T4, and T5 for theoretical and CFD findings are 5.75 per cent, 12.4 per cent, 15.45 per cent, and 15.5 per cent, respectively.

Table 4 shows that at 0.3 m/s velocity, the error values of T2, T3, T4, and T5 for theoretical and CFD findings are

Table 2. Comparison of temperature distribution at 0.1 m/s

Temperature (˚C)	T1	T2	T3	T4	T5
Theoretical	105	104.86	104.71	104.61	104.55
CFD	105	100.80	96.50	92.16	87.83

Table 3. Comparison of temperature distribution at 0.2 m/s

Temperature (˚C)	T1	T2	T3	T4	T5
Theoretical	105	94.25	84.37	77.78	74.1
CFD	105	100	96.4	92.00	87.7

Table 4. Comparison of temperature distribution at 0.3 m/s

Temperature (˚C)	T1	T2	T3	T4	T5
Theoretical	105	94.13	84.15	77.51	73.71
CFD	105	100.1	95.07	90.04	85.00

Table 5. Comparison of CFD results with theoretical for a Case 1

Results	h (W/m²K)	Nu	η (%)	ε
Theoretical	29.98	12.42	71.74	28.19
CFD	38.97	15.77	66.61	26.17

Table 6. Comparison of CFD results with theoretical for a Case 2

Results	h (W/m²K)	Nu	η (%)	ε
Theoretical	41.41	17.16	65.38	25.69
CFD	38.98	15.78	66.61	26.17

Table 7. Comparison of CFD results with theoretical for a Case 3

Results	h (W/m²K)	Nu	η (%)	ε
Theoretical	50.02	20.73	61.45	24.15
CFD	39.64	16.03	66.27	26.03

5.79 per cent, 11.48 per cent, 13.91 per cent, and 13.28 per cent, respectively.

Tables 5-7 shows the results of a comparison based on CFD and theoretical results for various cases using convective heat transfer coefficient, Nusselt number, Fin efficiency, and Fin effectiveness as performance parameters.

Table 5 shows that at 0.1 m/s velocity, the error values of h, Nu, η (%), and ε for theoretical and CFD findings are 23 per cent, 21.2 per cent, 7.5 per cent, and 7.71 per cent, respectively.

Table 6 shows that at 0.2 m/s velocity, the error values of h, Nu, η (%), and ε for theoretical and CFD findings are 6.2 per cent, 8.7 per cent, 1.8 per cent, and 1.8 per cent, respectively.

Table 7 shows that at 0.3 m/s velocity, the error values of h, Nu, η (%), and ε for theoretical and CFD findings are 26.1 per cent, 29.3 per cent, 7.27 per cent, and 7.2 per cent, respectively.

4.0 Conclusion

The current research focused on the flow and heat transfer characteristics evaluation of Pin-Fin using CFD and theoretical technique. The pin fin is made of brass and measures 1.2 cm in diameter and 12 cm in length. The Fin is enclosed by a rectangular duct measuring 15 cm X 10 cm X 100 cm. The primary purpose of this study is to compare the heat transfer coefficient, fin efficiency, and effectiveness at different Reynolds numbers with analytical analysis and CFD results. The temperature distribution across the fin for three separate cases indicates that as the flow fluid (air) velocity increases (0.1 m/s, 0.2 m/s, and 0.3 m/s), the temperature at various equivalent locations in the fin reduces in all three cases. When air flows over the surface of a fin, convection enhances the heat transfer rate and lowers the fin's surface temperature.

In three different cases, we established the theoretical

values of convective heat transfer coefficient, Fin efficiency, and Fin effectiveness as:

Case 1: 29.98 W/m^{2}K, 71.74% and 28.19, respectively.

Case 2: 41.41W/m^{2}K, 65.38% and 25.69, respectively.

Case 3: 50.02W/m^{2}K, 61.45% and 24.15, respectively.

In three different cases, CFD simulations provide the value of convective heat transfer coefficient, Fin efficiency, and Fin effectiveness as:

Case 1: 38.97W/m^{2}K, 66.61% and 26.17, respectively.

Case 2: 38.98W/m^{2}K, 66.61% and 26.17, respectively.

Case 3: 39.64W/m^{2}K, 66.27% and 26.03, respectively.

The outcome of the CFD simulation agrees well with the results of the analytical approach. The relative errors between the theoretical and CFD results for Case 2 are less than 9%, so the solution for this case is better compared.

5.0 Acknowledgment

We are grateful to VGST-KSTePS for funding to purchase a workstation and ANSYS software, which is utilised to complete the current simulation work.

6.0 References

1. Lee S. Optimum design and selection of heat sinks. Proc of 11th IEEE Semi-Ther Sym; 1995. p. 48-54.
2. Sergent J, Krum A. Thermal management handbook for electronic assemblies. First Edition, McGraw-Hill; 1998.
3. Yenkar RG, Quraishi IM, Irfan M. Experimental investigation of heat transfer intensification of pin fins under forced convection (A review). Int J Adv Struct Eng Mang Sci. 2016; 2(6):239-491.
4. Sahin B, Demir A. Performance analysis of a heat exchanger having perforated square fins. Appl Therm Eng. 2008; 28(5-6):621-32. https://doi.org/10.1016/j.applthermaleng.2007.04.003
5. Tahat M, Kodah ZH, Jarrah BA, Probert SD. Heat transfers from pin-fin arrays experiencing forced convection. Appl Energy. 2000; 67:419-442. https://doi.org/10.1016/S0306-2619(00)00032-5
6. Sahiti N, Durst F, Dewan A. Heat transfer enhancement by pin elements. Int J Heat Mass Transfer. 2005; 48(23-24):4738-47. https://doi.org/10.1016/j.ijheatmasstransfer.2005.07.001
7. Gunjalli CV, Satheesh J. Numerical Analysis and Performance Evaluation of Fin (ALHE30) material by using pin fin apparatus. Int J Res Inn Appl Sci. 2018 May; 3(5):01-06.
8. Bhargave AS. Forced convection heat transfer from extended surfaces with finned pins (Thesis). Virginia Polytechnic Institute, Blacksburg, Virginia; 1965.
9. Bilen K, Akyol U, Yapici S. Heat transfer and friction correlations and thermal performance analysis for a finned surface. Energy Convers Manag. 2001; 42(9):1071-83. https://doi.org/10.1016/S0196-8904(00)00119-9
10. Yu R, Chaoyi W, Shusheng Z. Transitional flow and heat transfer characteristics in a rectangular duct with stagger-arrayed short pin fins. Chinese J Aeronaut. 2009; 22(3):237-242. https://doi.org/10.1016/S1000-9361(08)60093-X
11. Tomar YS, Sahu MM. Comparative study of performance of pin fin under forced convection heat transfer. Int J Eng Res Tech. 2013; 2(9).
12. Osama K, Moataz A, Salaheldin H. Analytical and numerical study of heat transfer in fins. Int Res J Eng Tech. 2021; 8(1):1427-32.
13. Sharma SK, Sharma V. Maximising the heat transfer through fins using CFD as a tool. Int J Rec Adv Mech Eng. 2013; 2(3):13-28. https://doi.org/10.14810/ijmech.2016.5302
14. Das Debdatta. Heat transfer analysis of pin fin array. Conference: International Conference on Mechanical Engineering and Renewable Energy 2013, Chittagong University of Engineering and Technology; 2014.
15. Qin YZ, Darus AN, Che Sidik NA. Numerical analysis on natural convection heat transfer of a heat sink with cylindrical pin fin. J Adv Res Fluid Mech Therm Sci. 2014; 2(1):13-22.
16. Chamoli S, Chauhan R, Thakur NS. Numerical analysis of heat transfer and thermal performance analysis of surface with circular profile fins. Int J Energy Eng. 2011; 1(1):11-18.
17. Hanamant SD, Vijaykumar KN, Kavita D. Natural convection heat transfer flow visualization of perforated fin arrays by CFD simulation. Int J Res Eng Technology. 2013; 2(12):483-490. https://doi.org/10.15623/ijret.2013.0212081
18. Kumar MVHS. Experimental analysis of natural and forced convective heat transfer through cylindrical pin fin; 2018.

19. Watson AG. The contribution of conveyed coal to mine heat problems (Thesis). University of Nottingham for the degree of Doctor of Philosophy; 1981.
20. Prasad N, Lal B. Analysis of heat stress in an underground coal mine using computational fluid dynamics. Curr Sci. 2021; 121(2):264-74. https://doi.org/10.18520/cs/v121/i2/264-274
21. Kanam OH, Ahmed MO. A review on underground mine ventilation system. J Mines Met Fuels. 2021; 69(2):62-70. https://doi.org/10.18311/jmmf/2021/27334
22. De Felipe JJ, Vives-Costa J, Niubó M, Sanmiquel L. Experimental assessment of an analytical model of the convective heat transfer coefficient in a mine gallery. Min Metall Explor. 2022; 39:969-81. https://doi.org/10.1007/s42461-022-00593-1
23. Wagner H. The management of heat flow in deep mines. Min Rep. 2013; 149:88-100. https://doi.org/10.1002/mire.201300014
24. Yadav R. Heat and Mass Transfer. Central Publishing house, Allahabad; 2014.
25. Ali A, Mohammed N, Shakir A. Numerical investigation for enhancement of heat transfer in internally finned tubes using ANSYS CFX program. Basrah J Eng Sci. 2016; 16(2):89-99. https://doi.org/10.33971/bjes.16.2.9